

INTERVAL VALUED FUZZY MODELING AND INDIRECT ADAPTIVE CONTROL OF QUADROTOR

A PREPRINT

✉ **Moufid Bouhental***

LAAAS, Department of Electronics Engineering
Mostefa Ben Boulaïd University
Batna, Algeria
bouhentalam@gmail.com

✉ **Mouna Ghanai**

Department of Electronics Engineering
Mostefa Ben Boulaïd University
m.ghanai@univ-batna2.dz

✉ **Kheireddine Chafaa**

Department of Electronics Engineering
Mostefa Ben Boulaïd University
chafaak@gmail.com

December 8, 2022

ABSTRACT

In this paper, a combination of fuzzy clustering estimation and sliding mode control is used to control a quadrotor system, whose mathematical model is complex and has unknown elements, including structure, parameters, and so on. In addition, they may be affected by external environmental disturbances. At first, the nonlinear unknown part of the system is estimated by a fuzzy model, A new method is presented for constructing a Takagi-Sugeno (TS) interval-valued fuzzy model (IVFM) based on input-output data of the identified system. Following the construction of the fuzzy model that estimates the unknown part of the quadrotor system, a control and on-line adjusting of the fuzzy modeled part of dynamics is used. In this step, the system model will be estimated in adaptive form so that the dynamic equations can be used in sliding mode control. Finally, the proposed technique is applied, and the simulation results are presented to show the effectiveness of this approach in controlling the quadrotor with unknown nonlinear dynamics.

Keywords Interval values Modeling · fuzzy clustering · fuzzy control · Indirect adaptive control · quadrotor control · sliding mode control · type-2 fuzzy sets.

1 Introduction

The quadrotor unmanned aerial vehicle (UAV) is a typical second-order, nonlinear, strongly coupled dynamic system. An adaptive control scheme is significant for unmanned quadrotor helicopters, and this has received attention in the literature. External disturbances can have a impact on the stability and reliability of these systems. Therefore, it is very important to study the effects of system disturbances and design control strategies that address actuator faults and disturbances. To date, many methods and strategies have been presented in the literature H.Mo and Farid [2019]. Authors presents PD control as well as a fuzzy adaptive PD control scheme in which the controller's gains are automatically adjusted in relation to the error signal rate Gao et al. [2015]. The fuzzy adaptive PD controller is quicker at achieving the desired response as compared to the other one. The authors of Rabhi et al. [2011] used a robust fuzzy control approach to stabilize a quadrotor's attitude angles. They used the parallel distributed compensation technique to design the fuzzy controller. High-order sliding mode observer was designed to provide state information

*Use footnote for providing further information about author (webpage, alternative address)—*not* for acknowledging funding agencies.

required for fuzzy controller design. The study Niroumand and Seyedsajadi [2013], integrated integral backstepping with fuzzy logic to improve the flight controller's performance. Simulation results show superior performances for the fuzzy-integral backstepping approach over conventional integral backstepping. Fuzzy based sliding mode control for quadrotor UAV has recently been reported in Pazooki and Mazinan [2017] and control structure is augmented via a genetic algorithm for optimization purposes. This approach can be further investigated using second order sliding mode control to avoid chattering. In Ul Amin and Kamsin [2017], NRBF and E-RBF are used collectively to approximate the unknown dynamics of the quadrotor. A study Dierks and Jagannathan [2010], addresses online learning of the dynamics of a quadrotor nonlinear model through neural networks. Online learning is normally preferred over offline learning for the reason that quadrotors may fly in a dynamic environment where different worse case perturbations may occur, and such operating scenarios are hard to generate offline. Also, this study conveys the idea of using NNs to control the six degrees of freedom of a quadrotor along with designing an ANN observer to estimate states of the system. A neural network is used to approximate unmodeled dynamics during flight in Dierks and Jagannathan [2009], and interconnection errors in flight formation are investigated. In Li and Zheng [2016] the position controller considered as nonlinear system and approximated using radial basis function neural networks, This study is unique in a sense that a complete controller is approximated via adaptive rule and trained online. This neuronal network-based controller provides adaptation for parametric uncertainties along with other external disturbances. In Lee [2021] authors proposed a nonlinear-sliding-surface-based SMC for tracking and stabilization with an SMO. To improve the performance of the quadrotor system, they remodeled the augmented quadrotor dynamics and estimated the unmeasured states and their derivatives through the sliding mode observer. To improve the SMC control performance, a nonlinear sliding surface is used to reduce the convergence time with a modified deceleration curve. The authors proved the performance of a tracking system. Based on the above research analysis, we propose an adaptive control strategy, and design an adaptive controller for a quadrotor UAVs in the presence of external and internal disturbances. The introduced adaptive control strategy is based on fuzzy logic control theory and adaptive sliding mode theory. A new method for constructing a Takagi-Sugeno (TS) type-2 fuzzy model offline, based on input-output data, is proposed, and the obtained fuzzy model of the dynamic is used to build the model-based control of the system. with an adaptive control strategy scheme that compensates the effects of the disturbance and an unmodeled dynamics control system. The system's global asymptotic stability is validated by the Lyapunov function. The effectiveness and feasibility of the proposed method are demonstrated by simulation studies of the unmanned vehicle. The rest of the paper is organized as follows. Section 2 describes the proposed method of IVFM construction from input-output datasets of the system. Section 3 presents the application of the proposed method to build the IVFM of the quadrotor. Section 4 presents the proposed control strategy based on fuzzy logic control and adaptive sliding mode for the quadrotor UAV under external disturbances and parameter changes. The stability analysis of the new methodology is validated by the Lyapunov function. The results of simulation studies that demonstrate the performance of the proposed adaptive fuzzy schemes are presented in Section 5. Finally, general conclusions and future work plans are provided.

2 Fuzzy modeling

The proposed method for constructing a Takagi-Sugeno (TS) type-2 fuzzy model, based on the input-output data of the identified system is constructed in three steps: (1) structure identification by fuzzy clustering; (2) envelope detection; and (3) parameter identification. In the structure identification phase, a clustering method based on the Gustafson-Kessel algorithm (GKCA) is used in order to detect the linear subsystems of the whole nonlinear system Babuska et al. [1998] (local linearization). Then, an envelope detection algorithm (EDA) based on the derivative concept is proposed to estimate both the upper and lower membership functions of the type-2 fuzzy membership function (T2MF) defined point-wise. In the parameter identification step, the least squares algorithm is applied to compute the best parameter values for the premises (Gaussians) and the consequences (straight lines) parameters.

2.1 Fuzzy Clustering overview

Clustering is the partitioning of data into subsets or groups based on similarities between the data. The main potential of clustering is to detect the underlying structure in data, not only for classification and pattern recognition, but for model reduction and optimization. To detect clusters of different geometrical shapes in a single data set, we used the Fuzzy Gustafson Kessel Clustering (FGK), which extends the standard fuzzy c-means algorithm by employing an adaptive distance norm Babuska and Verbruggen [1997], Gustafson and Kessel [1979], Filho and Serra [2016]. Each cluster has its own norm-inducing matrix, A_i , which yields the inner-product norm Eqn. (1) shown below:

$$D_{ikA}^2 = (\mathbf{x}_k - \mathbf{v}_i)^T A_i (\mathbf{x}_k - \mathbf{v}_i), \quad (1)$$

where $1 \leq i \leq c, 1 \leq k \leq N$. The matrices A_i are used as optimization variables in the $C - means$ functional, which will allow to each cluster to adapt the distance norm to the local topological structure of the data. Let A denote a c-tuple of the norm-inducing matrices: $A = (A_1, A_2, \dots, A_c)$. The objective functional of the GK algorithm is defined by:

$$J(\mathbf{X}, \mathbf{U}, \mathbf{V}, \mathbf{A}) = \sum_{i=1}^c \sum_{k=1}^N (\mu_{ik})^m D_{ikA}^2 \quad (2)$$

where N the number of data points, c the number of clusters, x_k the k^{th} data point, v_i the i^{th} cluster center, μ_{ik} the degree of membership of the k^{th} data in the i^{th} cluster, A_i the norm-inducing matrix of the i^{th} cluster and m is a weighting exponent that determines the fuzziness of the resulting clusters (typically $m = 2$). In our paper, the GKCA is applied in order to obtain the fuzzy partition matrix $U = [\mu_{ik}]_{c \times N}$, with $\mu_{ik} \in [0, 1]$ a membership degree.

2.2 Proposed envelope detection and estimation algorithm

The individual partitioning subsets μ_{ik} projected on the regressor X will define directly fuzzy regions, in which the data can be reasonably approximated by linear sub-models defined by clusters. Projection data can also make the fuzzy system easy to read by humans

2.2.1 Detection of lower and upper premise MF

In order to detect the fuzzy premise MFs (lower MF \underline{f} and the upper MF \bar{f}) we propose in what follows an approach called for Envelope Detection Algorithm (EDA) based on derivative concept. The algorithm is described in the following algorithm:

1) First, we interpolate the points linearly (dotted curve in Fig. 1 (a). between all segments $[y(i), y(i+1)]$ where i represents the data indices.

The third-level of heading follows the style of the second-level heading. 2) We compute the slopes between each successive data points $[y(i), y(i+1)]$ as:

$$d(i+1) = \frac{y(i+1) - y(i)}{x(i+1) - x(i)} \quad (3)$$

3) Two cases can arise:

- When the slope d in interval $[x(i), x(i+1)]$ is positive, then the point is considered as higher membership point and memorized with its indices as $(I_h, y_h(I_h))$, where $I_h = i+1$ represents the indices of the corresponding higher membership point y_h s.t. $y_h(I_h) = y(i+1)$.
- Otherwise, when the slope d in interval $[x(i), x(i+1)]$ is negative, then the point is considered as lower membership point and memorized with its indices as $(I_L, y_L(I_L))$, where $I_L = i+1$ represents the indices of the corresponding lower membership point y_L s.t. $y_L(I_L) = y(i+1)$.

By applying our method cited above, we show in Fig. 1 the shape of the obtained upper and lower envelopes, which represent the upper and lower type-2 MFs. The details of this technique are given in EDA Algorithm Bouhental et al. [2017]. This algorithm doesn't ensure the separation of envelopes; to do that, we can apply the same algorithm again for both the upper and lower sets. When we apply this algorithm to the initial set of points, we get two sets: \underline{f} and \bar{f} . Next, we use the same algorithm for both sets (\underline{f} and \bar{f}) to get another four sets. The proposed algorithm can be presented as the algorithm described here :

1. Applying ADE(initial set) gives two sets (\underline{f}, \bar{f})
2. make $i = j = 1$
3. $(\underline{f}_j, \bar{f}_i) = ADE(\text{initial set})$
4. Calculate the upper set \bar{f}
 - (a) Make $i = i + 1$
 - (b) $(\underline{f}_i, \bar{f}_i) = ADE(\bar{f})$

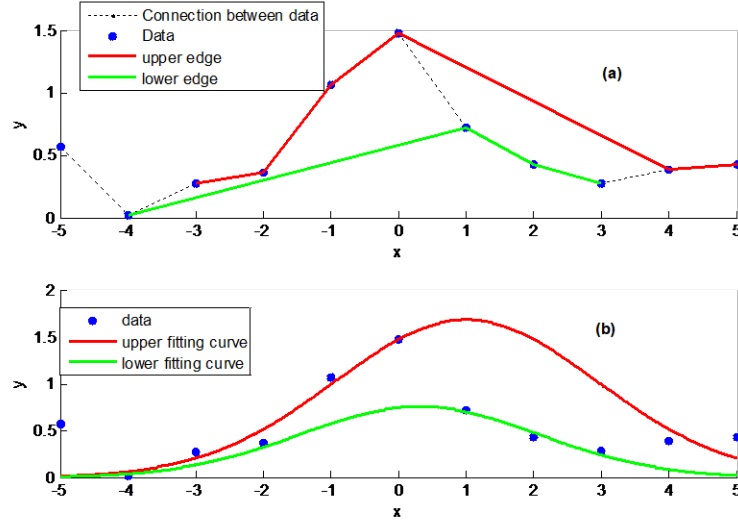


Figure 1: (a) Data envelope detection (b) Gaussian fitting

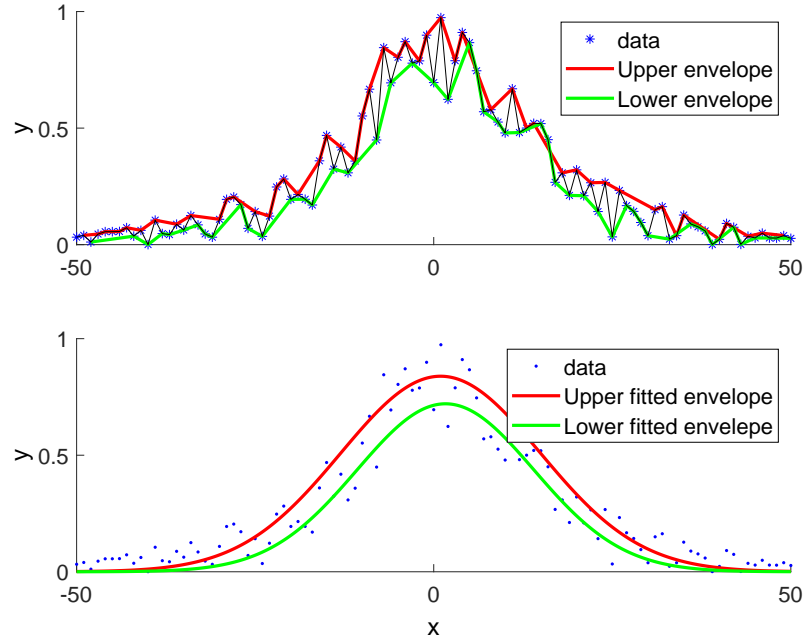


Figure 2: (a) with first applying EDA one time, (b) envelope fitting with Gaussian model

- (c) If go to step (a) else next:
- (d) $\bar{f} = \bar{f}_i$
- 5. Calculate the lower set
 - (a) Make $j = j + 1$
 - (b) $(\underline{f}_j, \bar{f}_j) = ADE(f)$
 - (c) If $j \neq j_{\max}$ go to step (a) else next:
 - (d) $\underline{f} = \underline{f}_j$

Look to the next example where the initial function is a Gaussian with added noise to create a cloud to its shape, in the Fig. 2 where the first ADE is applied and its corresponding fitting result as shown in the figure (b) there are many

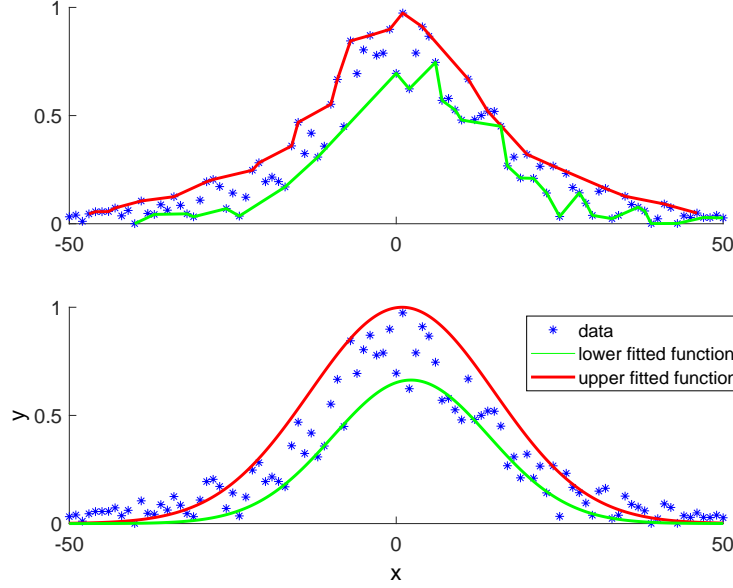


Figure 3: (c) after applying EDA two times, there are less intersection points (d) after Gaussian fitting, there is no intersection.

interactions points in different regions while the applying of EDA again make the envelopes less interacted and its fitted part show that our the final fitted functions envelopes much points of the initial cloud Fig. 3 (d).

2.3 Constructing fuzzy models from partitions

At this step, we have two data sets of points: data set 1 represents the data of f_L and data set 2 represents the data of f_U . Gaussian membership functions will be used in this investigation for the premise MF; thus, data sets 1 and 2 will be fitted to Gaussian models, yielding the lower and upper Gaussian membership functions \bar{f} and \underline{f} . Until now, we have obtained, by using the proposed method, type-2 fuzzy Gaussian membership functions for the premises. The global model can be conveniently represented as a set of affine Takagi-Sugeno (TS) rules R_i as follows:

$$\text{if } x \text{ is } \tilde{A}_i \text{ then } y_i = a_i x + b_i \text{ for } i = 1, 2, \dots, c \quad (4)$$

where x is the input, and y is the output, $\tilde{A}_i = [\underline{f}_i, \bar{f}_i]$ the i^{th} obtained antecedent type-2 fuzzy MF. The consequent parameters a_i and b_i are estimated from the data using least square method.

3 Fuzzy modeling of unknown dynamics of quadrotor

In the following application, we will use the method presented above to model the unknown functions using input-output data, and then we will use those initial models to build the adaptive control.

3.1 Dynamic model of Quadrotor

Let's consider the system in Eqn. (5) as presented in Lee [2021], Bouabdallah [2007] in which the state representation $\underline{x} = (\varphi, \dot{\varphi}, \theta, \dot{\theta}, \psi, \dot{\psi}, x, \dot{x}, y, \dot{y}, z, \dot{z})$ is the state vector and $U = [U_\phi \ U_\theta \ U_\psi \ U_z]$ is the control vector. The transformation matrix between the rate of change of the orientation angles $(\dot{\varphi}, \dot{\theta}, \dot{\psi})$ and the body angular velocities (p, q, r) can be considered as unity matrix if the perturbations from hover flight are small. Then, one can write $(\dot{\varphi}, \dot{\theta}, \dot{\psi}) \approx (p, q, r)$ Bouabdallah [2007]. Each axis can be approximately decoupled and controlled independently when the angular

Table 1: Parameters of the Quadrotor

$I_{zz} = 0.09kg.m^2$	$m = 1.2kg$	$l = 0.23m$
$I_{yy} = 0.18kg.m^2$	$d = 1.1e - 6N.m.s^2$	$g = 9.81m.s^{-2}$
$I_{xx} = 0.18kg.m^2$	$b = 54.2e - 6N.m^2$	$j_r = 1.32e - 3kg.m^2$

velocities are low and the attitude angle changes in small range. The drone parameters are shown in the Table 1.

$$\dot{x} = \begin{pmatrix} \dot{\phi} \\ \dot{\theta}\psi a_1 + \dot{\theta}a_2\Omega_r + b_1U_1 \\ \dot{\theta} \\ \dot{\phi}\psi a_3 + \dot{\phi}a_4\Omega_r + b_2U_2 \\ \dot{\psi} \\ \dot{\theta}\phi a_5 + b_3U_3 \\ \dot{z} \\ g - (\cos\phi \cos\theta) \frac{U_z}{m} \\ \dot{x} \\ u_x \frac{U_z}{m} \\ \dot{y} \\ u_y \frac{U_z}{m} \end{pmatrix} \quad (5)$$

$$\left. \begin{array}{l} a_1 = (I_{yy} - I_{zz})/I_{xx} \\ a_2 = J_r/I_{xx} \\ a_3 = (I_{zz} - I_{xx})/I_{yy} \\ a_4 = J_r/I_{yy} \\ a_5 = (I_{xx} - I_{yy})/I_{zz} \end{array} \right| \begin{array}{l} b_1 = l/I_{xx} \\ b_2 = l/I_{yy} \\ b_3 = 1/I_{zz} \\ u_x = (c\phi s\theta c\psi - s\phi s\psi) \\ u_y = (c\phi s\theta s\psi - s\phi c\psi) \end{array}$$

the moment and force caused by the propeller are proportional to the square of the angular velocity. The inputs of each axis can be composed of the speed of the propeller and described as Bouabdallah [2007]:

$$\left. \begin{array}{l} U_\phi = (\Omega_1 - \Omega_3) \\ U_\theta = (\Omega_4 - \Omega_2) \end{array} \right| \begin{array}{l} U_\phi = (\Omega_1 + \Omega_3 - \Omega_2 - \Omega_4) \\ U_z = (\Omega_1 + \Omega_2 + \Omega_3 + \Omega_4) \end{array}$$

3.2 Interval values Fuzzy modeling

The model Eqn. (5) can be decomposed into three subsystems:

$$\begin{pmatrix} \dot{x}_1 \\ \dot{x}_2 \end{pmatrix} = \begin{pmatrix} \dot{\phi} \\ f_\phi(\dot{\theta}, \dot{\psi}) + g_1U_1 \end{pmatrix} \quad (6)$$

$$\begin{pmatrix} \dot{x}_3 \\ \dot{x}_4 \end{pmatrix} = \begin{pmatrix} \dot{\theta} \\ f_\theta + g_2U_2 \end{pmatrix} \quad (7)$$

$$\begin{pmatrix} \dot{x}_5 \\ \dot{x}_6 \end{pmatrix} = \begin{pmatrix} \dot{\psi} \\ f_\psi + g_3U_3 \end{pmatrix} \quad (8)$$

where $f_\phi(\dot{\theta}, \dot{\psi}, \Omega_r) = \dot{\phi}\psi a_1 + \dot{\phi}a_2\Omega_r$, $f_\theta(\dot{\theta}, \dot{\psi}, \Omega_r) = \dot{\theta}\phi a_3 + \dot{\theta}a_4\Omega_r$, $f_\psi(\dot{\theta}, \dot{\psi}, \Omega_r) = \dot{\theta}\psi a_5$ and $g_\phi = b_1$, $g_\theta = b_2$, $g_\psi = b_3$. The parameters g_1, g_2, g_3 and the functions f_ϕ, f_θ and f_ψ are considered as unknown functions, and they will be estimated as follow :

the first step is to identify the functions $f_i(x, \dot{\psi}, \Omega_r)$ and g_i where $\{i = \phi, \theta, \psi\}$ using clustering. \hat{f}_i can be written as an TS approximation of the form IVFM Eqn. (4) :

$$\begin{aligned} f_\phi(x) &= \hat{f}_\phi(x_8, x_{12}, \Omega_r, \theta_{f_\phi}) + \varepsilon = \theta_{f_\phi}^T \varphi_{f_\phi}(x) \\ f_\theta(x) &= \hat{f}_\theta(x_{10}, x_{12}, \Omega_r, \theta_{f_\theta}) + \varepsilon = \theta_{f_\theta}^T \varphi_{f_\theta}(x) \\ f_\psi(x) &= \hat{f}_\psi(x_{10}, x_{12}, \theta_{f_\psi}) + \varepsilon = \theta_{f_\psi}^T \varphi_{f_\psi}(x) \end{aligned}$$

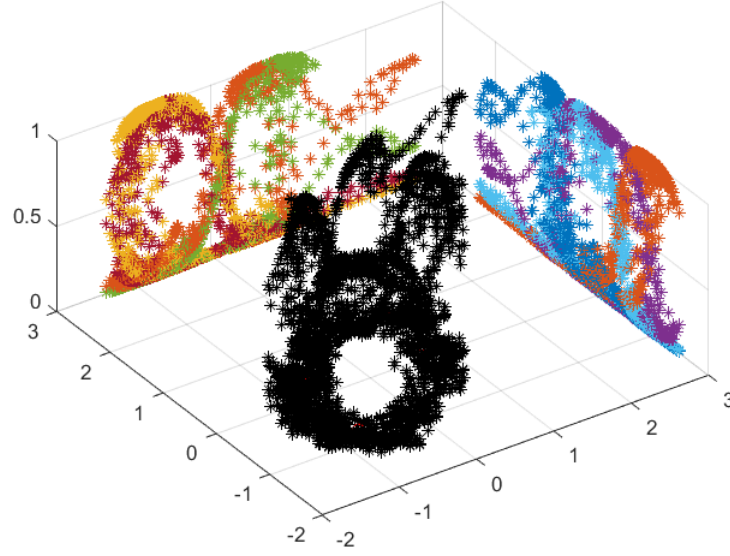
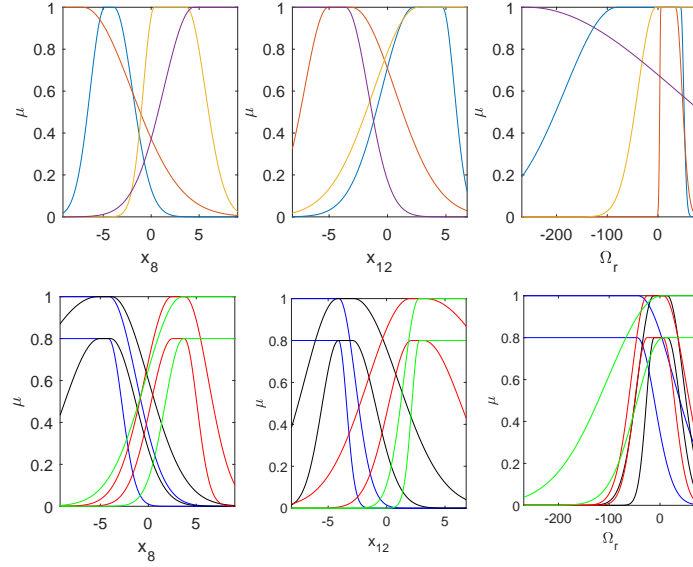


Figure 4: Projection and construction of membership functions

Figure 5: Membership Functions of $\hat{f}_\phi(\underline{x})$

where $\theta_{f_i} = [\underline{w}_l^T, \underline{w}_r^T]^T$ and $\underline{\psi}_{f_i}(x, \dot{x}) = \frac{1}{2} [\xi_l^T(x, \dot{x}), \xi_r^T(x, \dot{x})]^T$.

To collect input-output data, we generate two sets of data, one for identification by clustering, and the second for validation. We start with a sequence of 4000 samples (2000 for identification and 2000 for validation) The sampling time is $T = 0.01s$ with normal noise (05% of amplitude) is added to every output. The obtained data is treated using EDA in order to construct the membership functions as presented in Fig. 4. The membership functions type-1 and type-2 obtained with simulation data for $f_\phi(x, \Omega)$, $f_\theta(x, \Omega)$ and $f_\psi(x, \Omega)$ are depicted in The figures (Fig. 5, 7), respectively.

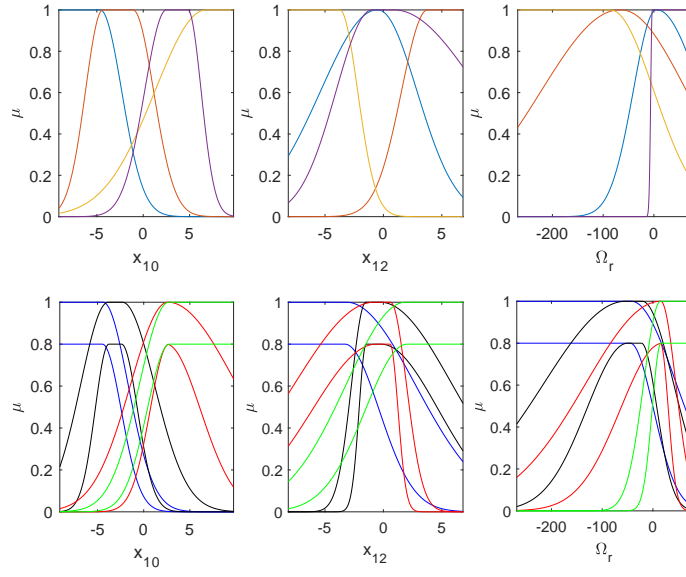
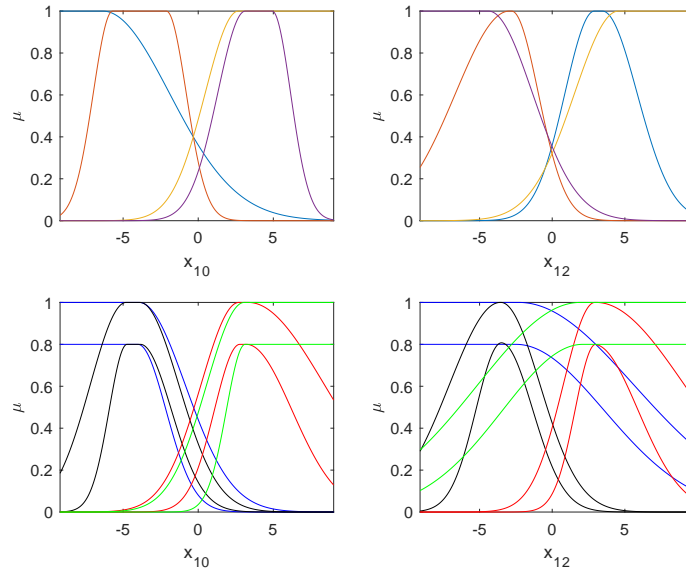
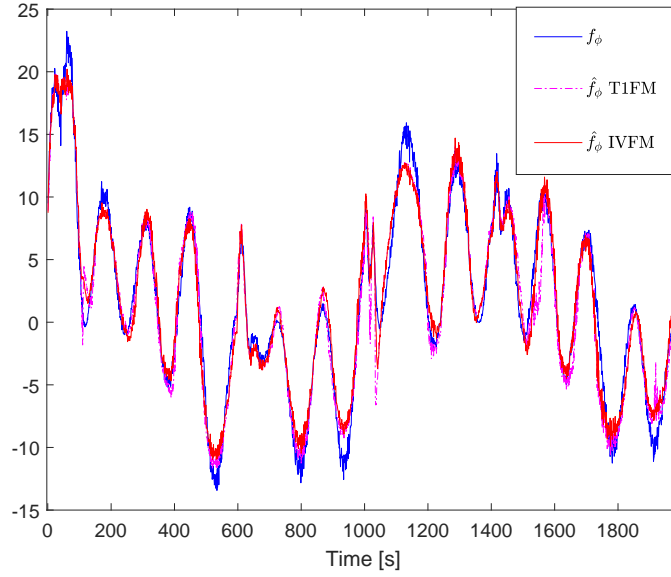
Figure 6: Membership Functions of $\hat{f}_\theta(x)$ Figure 7: Membership Functions of $\hat{f}_\psi(\underline{x})$

Table 2: Comparison between RMSE of T1FM and IVFM

$f_i(x, \Omega)$	$\hat{f}_i(x, \theta_{fi})$	T1FM	IVFM
$f_\phi(x, \Omega)$	$\hat{f}_\phi(x_8, x_{12}, \theta_{f_\phi})$	1.5958	1.4016
$f_\theta(x, \Omega)$	$\hat{f}_\theta(x_{10}, x_{12}, \theta_{f_\theta})$	1.1717	1.1009
$f_\psi(x, \Omega)$	$\hat{f}_\psi(x_{10}, x_{12}, \theta_{f_\psi})$	0.2072	0.1930

The validation of fuzzy models obtained (the fuzzy model type-2 ; IFVS and the fuzzy model type-1 ; T1FS) as shown in Fig. 8 9 10 and the Table 2 show that our proposed technique (IVFM) is more close to real functions of system compared to the type-1 model.

Figure 8: Comparaison between $\hat{f}_\phi(x)$ and $f_\phi(x)$

4 Indirect Adaptive control

The initial model of the antecedent part in Eqn. (4) plays an important role in the structure of the system. The previous clustering algorithm is used to build the initial structure of the unknown part of a nonlinear system with a fuzzy model. The laws of Lyapunov are then applied to adjust the identified model while maintaining system stability.

Let $\underline{e}(t) = \underline{x}_m(t) - \underline{x}(t)$ the error of tracking, $K = [k_0, 1]$ a vector of parameters of conception and the equation of sliding is given by:

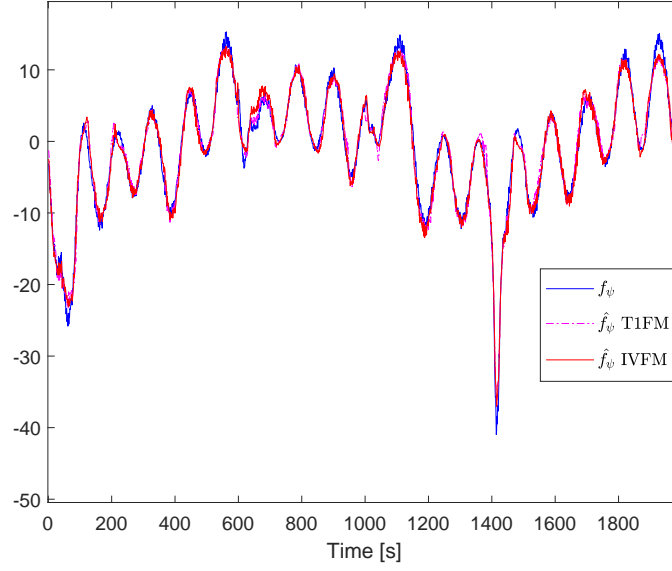
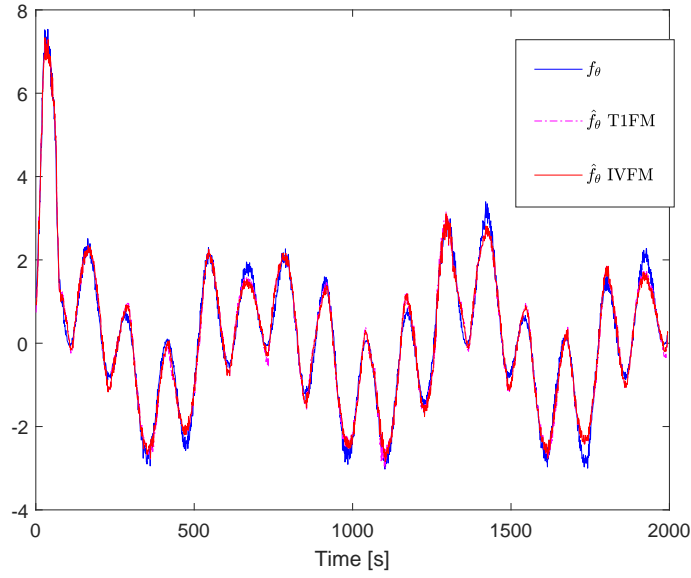
$$\underline{e}_s(t) = \underline{e} + k_0 \dot{\underline{e}} \quad (9)$$

where $e_s(t) = (e_{s_x}, e_{s_y}, e_{s_z}, e_{s_\theta}, e_{s_\phi}, e_{s_\psi})$ represent the sliding surface.

4.1 Design of fuzzy adaptive SMC control law

The approximated functions $f(x)$ and $g(x)$ with the universelle approximator flous, take the following forme: $\hat{f}(x, \theta) = \theta_f^T \varphi_f(x)$ and $\hat{g}(x, \theta) = \theta_g^T \varphi_g(x)$ With φ_f and φ_g are the basis of fuzzy vector functions, supposed convenablement fixed by the fuzzy identification presented in 3.2, and are the vectors of paramètres ajustables supposed définis respectively in the domaine Ω_f and Ω_g . We définie the sub-set $S_x \subseteq \mathbb{R}^n$ as a space in which the trajectoires of states x stay inside it in the closed loop. The functions $f(x)$ and $g(x)$ are written as follow :

$$\begin{aligned} \hat{f}(x, \theta_f) &= f^*(x, \theta_f^*) + w_f(x) \\ \hat{g}(x, \theta_g) &= g^*(x, \theta_g^*) + w_g(x) \end{aligned} \quad (10)$$

Figure 9: Comparaision between $\hat{f}_\theta(x)$ and $f_\theta(x)$ Figure 10: Comparaision between $\hat{f}_\psi(x)$ and $f_\psi(x)$

with w_f and w_g represente errors of apprximation. $f^*(x, \theta)$ and $g^*(x, \theta)$ are respectively the optimal parameters of $\hat{f}(x)$ and $\hat{g}(x)$. The values of paramètres θ_f and θ_g minimise respectively tthe errors of approximation $w_f(x)$ and $w_g(x)$. those optimal paramètres satisfy :

$$\begin{aligned}\theta_f^* &= \arg \min_{\theta_f \in \Omega_f} \left(\sup_{x \in S_x} \left| \theta_f^T \varphi_f(x) - f(x) \right| \right) \\ \theta_g^* &= \arg \min_{\theta_g \in \Omega_g} \left(\sup_{x \in S_x} \left| \theta_g^T \varphi_g(x) - g(x) \right| \right)\end{aligned}\tag{11}$$

We suppose that $|w_f(x)| \leq W_f$ and $|w_g(x)| \leq W_g$ where $W_f(x)$ and $W_g(x)$ are the known upper bound of approximation error. Both functions can be chosen arbitrarily small. The parameters of errors are :

$$\begin{aligned}\tilde{\theta}_f(t) &= \theta_f(t) - \theta_f^* \\ \tilde{\theta}_g(t) &= \theta_g(t) - \theta_g^*\end{aligned}\tag{12}$$

Considering the following proposed indirect fuzzy control

Both terms u_{eq} and u_s will be calculated with details in the next sections. In the following we note IVFC (Interval value fuzzy control) and IVFM (Interval value fuzzy Model) for the control based on type-2 fuzzy system, in other hand we note T1FC and T1FM for the model based on type-1 fuzzy and Type-2 fuzzy system respectively.

4.1.1 Terme of equivalence control u_{eq}

take $\bar{e}_s(t) = k_{d-2}e^{(d-1)}(t) + \dots + k_0\dot{e}(t)$ in order to have $\bar{e}_s(t) = \dot{e}_s(t) - e^{(d)}(t)$. The certainty equivalence control term Sastry and Isidori [1989] become as:

$$u_{eq} = -\frac{1}{\hat{g}(x)}(\hat{f}(x) + \nu(t))\tag{13}$$

where $\nu(t) = y_d^{(d)} + \gamma e_s + \bar{e}_s$ and $\gamma > 0$ is a design parameter. The d th derivative of the output error $e^{(d)} = y_d^{(d)} - y^{(d)}$ with $u = u_{eq} + u_s$, hence :

$$\begin{aligned}e^{(d)} &= y_d^{(d)} - f(x) - g(x)u(t) \\ &= y_d^{(d)} - f(x) - \frac{g(x)}{\hat{g}(x)}(-\hat{f}(x) + \nu(t)) - (g(x))u_s\end{aligned}\tag{14}$$

Note that the two first terms of the Eqn. (14):

$$\begin{aligned}y_d^{(d)} - f(x) &= y_d^{(d)} - \hat{f}(x) - f(x) + \hat{f}(x) \\ &= (-\hat{f}(x) + \nu(t)) - f(x) + \hat{f}(x) - \gamma e_s - \bar{e}_s\end{aligned}\tag{15}$$

We substitute Eqn. (15) in Eqn. (14), leads to :

$$\begin{aligned}e^{(d)} &= (\hat{f}(x) - f(x)) + (\hat{g}(x) - g(x))u_{eq} \\ &\quad - \gamma e_s - \bar{e}_s - g(x)u_s\end{aligned}\tag{16}$$

And with $\bar{e}_s = \dot{e}_s - e^{(d)}$, leads to :

$$\dot{e}_s + \gamma e_s = (\hat{f}(x) - f(x)) + (\hat{g}(x) - g(x))u_{eq} - (g(x))u_s$$

4.1.2 law of parameters adaptation

Consider the Lyapunov candidate function:

$$V_i = \frac{1}{2}e_s^2 + \frac{1}{2\eta_f}\tilde{\theta}_f^T\tilde{\theta}_f + \frac{1}{2\eta_g}\tilde{\theta}_g^T\tilde{\theta}_g\tag{17}$$

Where $\eta_f > 0$ and $\eta_g > 0$ are the parameters of conception. The derivative of Lyapunov function Eqn. (17), gives us:

$$\begin{aligned}\dot{V}_i &= e_s \left(-\gamma e_s + (\hat{f} - f) + (\hat{g} - g)u_{eq} - (g)u_s \right) \\ &\quad + \frac{1}{\eta_f}\tilde{\theta}_f^T\dot{\theta}_f + \frac{1}{\eta_g}\tilde{\theta}_g^T\dot{\theta}_g\end{aligned}\tag{18}$$

In other hand ,

$$\begin{aligned}\hat{f} - f &= \theta_f^T\phi_f(x) - \theta_f^{*T}\phi_f(x) - w_f(x) \\ &= \tilde{\theta}_f^T\phi_f(x) - w_f(x)\end{aligned}\tag{19}$$

Same thing with $(\hat{g} - g)$ hence,

$$\begin{aligned} \dot{V}_i = & + \left(\tilde{\theta}_f^T \phi_f - w_f + \tilde{\theta}_g^T \phi_g u_{eq} - w_g u_{ce} - g u_s \right) e_s \\ & + \frac{1}{\eta_f} \tilde{\theta}_f^T \dot{\theta}_f + \frac{1}{\eta_g} \tilde{\theta}_g^T \dot{\theta}_g - \gamma e_s^2 \end{aligned} \quad (20)$$

We choose the following adaptation laws :

$$\begin{aligned} \dot{\theta}_f(t) &= -\eta_f \varphi_f(x) e_s \\ \dot{\theta}_g(t) &= -\eta_g \varphi_g(x) e_s u_{eq} \end{aligned} \quad (21)$$

where $\varphi_f(x) = \frac{1}{2} (\xi_l^f + \xi_r^f)$ and $\varphi_g(x) = \frac{1}{2} (\xi_l^g + \xi_r^g)$, the speed of adaptation related to the choice of the values of η_f and η_g . we suppose that the ideal parameters are constants $\dot{\theta}_f = \dot{\theta}_f^*$ and $\dot{\theta}_g = \dot{\theta}_g^*$. With those conditions we find that: $\frac{1}{\eta_g} \tilde{\theta}_g^T \dot{\theta}_g = -\tilde{\theta}_g^T \varphi_g(x) e_s u_{eq}$ and $\frac{1}{\eta_f} \tilde{\theta}_f^T \dot{\theta}_f = -\tilde{\theta}_f^T \varphi_f(x) e_s$ hence,

$$\dot{V}_i = -\gamma e_s^2 + (-w_f(x) - w_g(x) u_{eq} - g(x) u_s) e_s \quad (22)$$

4.1.3 Projection Modification to Parameter's Update Laws

The laws of adaptation in the equations (18-19) don't guaranty that $\theta_f \in \Omega_f$ and $\theta_g \in \Omega_g$. We must use the projection to insure that (e.g. to guaranty that $\hat{g}(x) \geq g_0$). We suppose in particular that the i^{th} component of θ_f^* and θ_g^* is in the known interval: $\theta_{f_i}^* \in [\theta_{f_i}^{\min}, \theta_{f_i}^{\max}]$ and $\theta_{g_i}^* \in [\theta_{g_i}^{\min}, \theta_{g_i}^{\max}]$ and we want that and, we define as a point in the acceptable region. We can resume this algorithm by using the following rule : if $\theta_f(t) \notin [\theta_f^{\min}, \theta_f^{\max}]$ and $\theta_f^{ud}(\theta_f - \theta_f^n) \geq 0$ then $\dot{\theta}_f(t) = 0$ else $\dot{\theta}_f(t) = -\eta_f \varphi_f e_s u_{eq}$

In the stability analysis, this projection modification to the update laws will always result in a parameter estimation error that will decrease V_i at least as much as if the projection were not used; hence, the right-hand side of Eqn. (22) will overbound the \dot{V}_i that would result if projection is used. For this reason, we conclude that:

$$\dot{V}_i \leq -\gamma e_s^2 + (-w_f(x) - w_g(x) u_{eq} - g(x) u_s) e_s \quad (23)$$

4.1.4 Sliding Mode Control Term

To ensure that Equation Eqn. (23) is less than or equal to zero, we choose:

$$u_s = \eta(x) \operatorname{sgn}(e_s) = \frac{1}{g_0} (W_f(x) + W_g(x) |u_{eq}|) \operatorname{sgn}(e_s)$$

We see that : $-(w_f(x) + w_g(x) u_{eq}) e_s \leq (|w_f(x)| + |w_g(x) u_{eq}|) |e_s|$ with $\frac{g(x)}{g_0} \geq 1$ hence:

$$\begin{aligned} \dot{V}_i \leq & -\gamma e_s^2 + (|w_f(x)| + |w_g(x) u_{eq}|) |e_s| \\ & - e_s \frac{g}{g_0} (W_f(x) + W_g(x) |u_{eq}|) \operatorname{sgn}(e_s) \end{aligned} \quad (24)$$

$$\begin{aligned} \dot{V}_i \leq & -\gamma e_s^2 + |w_f(x)| |e_s| + |w_g(x) u_{eq}| |e_s| \\ & - e_s \operatorname{sgn}(e_s) W_f(x) - e_s \operatorname{sgn}(e_s) W_g(x) |u_{eq}| \end{aligned} \quad (25)$$

where $|e_s| = e_s \operatorname{sgn}(e_s)$, $\forall e_s \neq 0$: and $|w_g(x)| \leq W_g(x)$ then :

$$\begin{aligned} |w_f(x)| |e_s| - e_s \operatorname{sgn}(e_s) W_f(x) &= |e_s| (|w_f(x)| - W_f(x)) \leq 0 \\ |w_g(x) u_{eq}| |e_s| - e_s \operatorname{sgn}(e_s) W_g(x) |u_{eq}| &= \\ |e_s| (|w_g(x) u_{eq}| - W_g(x) |u_{eq}|) &\leq 0 \\ \dot{V}_i \leq & -\gamma e_s^2 \end{aligned} \quad (26)$$

because $\gamma e_s^2 \geq 0$, this show that \dot{V}_i which is a measure of the tracking error and parameter estimation error, is a nonincreasing function of time. Notice that $\gamma > 0$ has an influence on how fast $V_i \mapsto 0$. By picking γ larger you will often get faster convergence of the tracking error.

4.1.5 Asymptotic Convergence of the Tracking Error and Boundedness of Signals

Due the hypothesis considered (that the reference signals are bounded, x is measurable, $d = n$, and the projection ensures that the u_{eq} term is well-defined), the following statements hold:

1. The system output $y, \dot{y}, \dots, y^{(d-1)}$ are bounded
2. The control signal u, u_{eq} et u_s are bounded.
3. The parameteres $\theta_g(t)$ and $\theta_f(t)$ are bounded.
4. The magnitude of the output error decreases at least asymptotically to zero ($\lim_{t \rightarrow \infty} e(t) = 0$)

To prove this, Note that since V_i is positive and $\dot{V}_i \leq -\gamma e_s^2$. We know that e_s, θ_f and θ_g are bounded. since e_s is bounded and y_r and its derevatives are bounded. We know that $y, \dot{y}, \dots, y^{(d-1)}$ are bounded. Hence, x are bounded. Hence, $f(x), \hat{f}(x), g(x)$ and $\hat{g}(x)$ are bounded. Since x is bounded and $\hat{g}(x) \geq g_0$, u_{eq} and u_s and hence u , are bounded. Next, note that :

$$\int_0^\infty \gamma e_s^2 dt \leq - \int V_i dt = V_i(0) - V_i(\infty) \quad (27)$$

This establishes that $e_s \in L_2$ ou $L_2 = \{z(t) : \int_0^\infty z^2(t) dt < \infty\}$ since $V_i(0)$ and $V_i(\infty)$ are bounded. Note that via the equation (15), \dot{e}_s is bounded. Hence, because \dot{e}_s and e_s are bounded and $e_s \in L_2$, and via the barbarat's lemma we have $\lim_{t \rightarrow \infty} e_s(t) = 0$. Hence $\lim_{t \rightarrow \infty} e(t) = 0$.

It is possible to reduce the chattering that can be result in the sliding mode term of control, we introduce $e_\varepsilon = (e_{\varepsilon_x}, e_{\varepsilon_y}, e_{\varepsilon_z}, e_{\varepsilon_\theta}, e_{\varepsilon_\varphi}, e_{\varepsilon_\psi})$ we can use the smooth function $\text{sgn}(e_s)$ Slotine and Coetsee [1986]. In this case, however, you only get convergence to an neighborhood of $e_s = 0$. To prove the stability, we define the error e_ε .

$$e_\varepsilon = e_s - \varepsilon \text{sat}\left(\frac{e_s}{\varepsilon}\right) \quad (28)$$

where

$$\text{sat}(x) = \begin{cases} 1 & \text{si } 1 \leq x \\ x & \text{si } -1 < x < 1 \\ -1 & \text{si } x \leq -1 \end{cases}$$

where e_ε represent the distance between e_s and the desired “boundary layer,” so the $e_\varepsilon = 0$ when e_s is inside the layer. The equivalent control is defined to be:

$$u_{eq} = -\frac{1}{\hat{g}(x)}(\hat{f}(x) + \nu_\varepsilon(t)) \text{ with } \nu_\varepsilon(t) = y_d^{(n)} + \gamma e_\varepsilon + \bar{e}_s$$

we consider the following lyapunouv function:

$$V_i = \frac{1}{2} e_\varepsilon^2 + \frac{1}{2\eta_f} \tilde{\theta}_f^T \tilde{\theta}_f + \frac{1}{2\eta_g} \tilde{\theta}_g^T \tilde{\theta}_g$$

And the Adaptation laws became :

$$\begin{aligned} \dot{\theta}_f(t) &= -\eta_f \varphi_f(x) e_\varepsilon \\ \dot{\theta}_g(t) &= -\eta_g \varphi_g(x) e_\varepsilon u_{eq} \end{aligned} \quad (29)$$

with those laws the derived lyapunov functions:

$$\dot{V}_i \leq -\gamma e_\varepsilon^2 + (|w_f(x)| + |w_g(x) u_{ce}|) |e_\varepsilon| - g(x) u_s e_\varepsilon$$

the terme u_s in Eqn. (30) become a control with smooth action.

$$u_s = \frac{1}{g_0} (W_f(x) + W_g(x) |u_{eq}|) \text{sat}\left(\frac{e_s}{\varepsilon}\right) \quad (30)$$

with $e_\varepsilon \text{sat}(\frac{e_s}{\varepsilon}) = |e_\varepsilon|$, we can proof that $\dot{V}_i \leq -\gamma e_\varepsilon^2$, that's make $|e_\varepsilon|$ asymptotically stable, in addition e_s will converge to the ε -neighbor of $e_s = 0$, and e will converge to 0.

4.2 Control of position and attitude of Quadrotor

Proposition 1: for the conception of attitude controller described by the following sub-systems (6), (7) and (8).

we propose a sliding mode controller for every subsystem i where $i = \{\phi, \theta, \psi\}$ as follow:

$$U_i = u_{eq_i} + u_{s_i} \quad (31)$$

where :

$$u_{eq_i} = -\frac{1}{\hat{g}_i(x)} \left(\hat{f}_i(x, \theta_{f_i}) + \ddot{y}_{d_i} + \gamma e_{\varepsilon_i} + \bar{e}_{s_i} \right)$$

$$u_{s_i} = \frac{1}{g_{0i}} (W_{f_i}(x) + W_{g_i}(x) |u_{eq_i}|) \text{sat}\left(\frac{e_{s_i}}{\varepsilon}\right)$$

where $\bar{e}_s = k_i e$, $y_{d_i} = \{\phi_d, \varphi_d, \theta_d\}$, $d = 2$, $W_{f_i}(x)$ and $W_{g_i}(x)$ are the errors bounds of the approximation of f_i and g_i respectively. with g_{0i} is the minimum value of b_i . the control input Eqn. (31) ensures the asymptotic convergence of ϕ, θ and ψ to ϕ_d, θ_d, ψ_d respectively.

Proof : similarly, to sections 4.1.1 and 4.1.4, we take $n = 2$, the equations Eqn. (13) and Eqn. (30) became:

$$U_i = \frac{1}{\hat{b}_i} \left(-\hat{f}_i(x, \varphi_{f_i}) + \gamma e_{\varepsilon_i} + \bar{e}_{s_i} + \ddot{y}_{i_d} \right) + \frac{1}{g_{0i}} (W_{f_\phi}(x) + W_{g_i}(x) |u_{eq_i}|) \text{sat}\left(\frac{e_{s\phi}}{\varepsilon}\right) \quad (32)$$

using the equations in Eqn. (29), the adaptations laws can be written as follow:

$$\dot{\theta}_{f_i} = -\eta_{f_i} \varphi_{f_i}(x) e_{\varepsilon_i}$$

$$\dot{\theta}_{g_i} = -\eta_{g_i} e_{\varepsilon_i} u_{eq_i} \quad (33)$$

Notice that the functions g_i in Eqn. (33) is considered as a constants that's why it is approximated with a constant and not a fuzzy function, so we take $\varphi_{f_i} = 1$.

Proposition 2 : for the altitude controller, the subsystem that governs the movement $z(t)$ is :

$$\begin{pmatrix} \dot{x}_7 \\ \dot{x}_8 \end{pmatrix} = \begin{pmatrix} \dot{z} \\ f_z - U g_z U_z \end{pmatrix}$$

where $U = (\cos \phi \cos \theta)$, $g_z = \frac{1}{m}$ and f_z is the gravity g . The sliding mode control Eqn. (34) ensure the convergence of $z(t)$ toward the consign z_d

$$U_z = \frac{1}{U g_z} (-\hat{f}_z(x) + \ddot{z}_d + \gamma e_{\varepsilon_z} + \bar{e}_{s_z}) + \frac{1}{g_0} (W_{f_z}(x)/(U) + W_{g_z}(x) |u_{eq_z}|) \text{sat}\left(\frac{e_{sz}}{\varepsilon}\right) \quad (34)$$

Where $W_{f_z}(x)$ and $W_{g_z}(x)$ are the bounded limit of error of the approximation of f_z and g_z respectively

Proof : following the same procedure in the sections 4.1.1 and 4.1.4, considering $\ddot{z} = \ddot{f}_4(x) - U g_z U_z(t)$ where , the term of equivalent control is defined as :

$$u_{eq_z} = -\frac{1}{U g_z} \left(\hat{f}_z(x | \theta_{f_z}) + \ddot{z}_d + \gamma e_{\varepsilon_z} + \bar{e}_{s_z} \right)$$

where $\nu(t) = \ddot{z}_d + \gamma e_{s_z} + \bar{e}_{s_z}$ and $\gamma > 0$

The 2^{end} derivative of the output error, along with the equation Eqn. (14) we can write:

$$\ddot{e} = \ddot{z}_d - f_z(x) - \frac{g_z}{g_z} \left(-\hat{f}_z(x) + \nu(t) \right) - U g_z u_s \quad (35)$$

Take the two first terms as follow:

$$\ddot{z}_d - f_z(x) = \left(-\hat{f}_z(x) + \nu(t) \right) - f_z(x) + \hat{f}_z(x) - \gamma e_{s_z} - \bar{e}_{s_z}$$

we substitute both terms in the equation Eqn. (35), using $\bar{e}_s = \dot{e}_s - e^{(d)}$ we find:

$$\dot{e}_s + \gamma e_s = (\hat{f}_z - f_z) + (\hat{g}_z - g_z)U u_{eq_z} - U g u_s$$

The candidate function of Lyapunov V_i :

$$V_z = \frac{1}{2} e_{\varepsilon_z}^2 + \frac{1}{2\eta_f} \tilde{\theta}_{f_z}^T \tilde{\theta}_{f_z} + \frac{1}{2\eta_g} \tilde{\theta}_{g_z}^T \tilde{\theta}_{g_z}$$

where $\eta_f > 0$ and $\eta_g > 0$ are the adaptation gain. the derivative of V_i gives us:

$$\begin{aligned} \dot{V}_z &= (\tilde{\theta}_{f_z}^T \phi_f - w_{f_z} + U \tilde{\theta}_{g_z}^T \phi_g u_{eq_z} - U w_g u_{eq_z} - U g u_s) e_{\varepsilon_z} \\ &\quad - \gamma e_{\varepsilon_z}^2 + \frac{1}{\eta_f} \tilde{\theta}_f^T \dot{\theta}_f + \frac{1}{\eta_g} \tilde{\theta}_g^T \dot{\theta}_g \end{aligned} \quad (36)$$

Suppose that those ideal parameters are constants $\dot{\theta}_f = \dot{\theta}_f$ and $\dot{\theta}_g = \dot{\theta}_g$, and the chosen adaptation law is:

$$\begin{aligned} \dot{\theta}_{f_z}(t) &= -\eta_{f_z} \varphi_{f_z}(x) e_{\varepsilon_z} \\ \dot{\theta}_{g_z}(t) &= -\eta_{g_z} \varphi_{g_z}(x) e_{\varepsilon_z} u_{eq_z} (\cos \phi \cos \theta) \end{aligned}$$

That's lead to: $\frac{1}{\eta_g} \tilde{\theta}_g^T \dot{\theta}_g = -\tilde{\theta}_g^T \varphi_g(x) e_{\varepsilon_z} u_{eq}$ and $\frac{1}{\eta_f} \tilde{\theta}_f^T \dot{\theta}_f = -\tilde{\theta}_f^T \varphi_f(x) e_{\varepsilon_z}$, so the equation Eqn. (36) can be written as:

$$\dot{V}_z = -\gamma e_{\varepsilon_z}^2 + (-w_{f_z}(x) - U w_g(x) u_{eq_z} - U g(x) u_s) e_{\varepsilon_z}$$

To analyze the stability, we conclude that:

$$\dot{V}_z \leq -\gamma e_{\varepsilon_z}^2 + (-w_{f_z}(x) - U w_{g_z}(x) u_{eq_z} - U g(x) u_s) e_{\varepsilon_z} \quad (37)$$

To ensure that the equation Eqn. (37) must be less than or equal to zero, we choose:

$$u_s = \frac{1}{g_0} \left(\frac{W_{f_z}(x)}{U_1} + W_{g_z}(x) |u_{eq_z}| \right) \text{sat}\left(\frac{e_s}{\varepsilon}\right) = \eta(x) \text{sat}\left(\frac{e_s}{\varepsilon}\right)$$

We note that: $-(w_{f_z}(x) + w_g(x) u_{eq}) e_s \leq (|w_{f_z}(x)| + |w_g(x) u_{eq}|) |e_s|$, so:

$$\begin{aligned} \dot{V}_z &= -\gamma e_s^2 + (-w_{f_z}(x) - U w_{g_z}(x) u_{eq_z} \\ &\quad - U \frac{g_z(x)}{g_{0z}} \left(\frac{W_{f_z}(x)}{U} + W_{g_z}(x) |u_{eq_z}| \right) \text{sat}\left(\frac{e_s}{\varepsilon}\right)) e_{\varepsilon} \end{aligned} \quad (38)$$

$$\begin{aligned} \dot{V}_z &\leq -\gamma e_{\varepsilon_z}^2 + (|w_{f_z}(x)| + |U w_{g_z}(x) u_{eq_z}|) |e_{\varepsilon_z}| \\ &\quad - U e_{\varepsilon_z} g_z(x) \left(\frac{1}{g_{0z}} \left(\frac{W_{f_z}(x)}{U} + W_g(x) |u_{eq_z}| \right) \text{sat}\left(\frac{e_s}{\varepsilon}\right) \right) \end{aligned} \quad (39)$$

Now, we consider the last term of the equation Eqn. (39) and because $\frac{g_z(x)}{g_{0z}} \geq 1$ so :

$$\begin{aligned} \dot{V}_i &= -\gamma e_{\varepsilon_z}^2 + |w_{f_z}(x)| |e_s| - e_{\varepsilon} \text{sat}\left(\frac{e_s}{\varepsilon}\right) W_{f_z}(x) \\ &\quad + |U w_{g_z}(x) u_{eq_z}| |e_{\varepsilon}| - U e_{\varepsilon} \text{sat}\left(\frac{e_s}{\varepsilon}\right) W_{g_z}(x) |u_{eq_z}| \end{aligned} \quad (40)$$

with $|e_\varepsilon| = e_s \text{sat}(e_s/\varepsilon)$, $|w_f(x)| \leq W_f(x)$ and $|w_g(x)| \leq W_g(x)$ so:

$$\begin{aligned} |w_{f_z}(x)| |e_\varepsilon| - e_\varepsilon \text{sat}\left(\frac{e_s}{\varepsilon}\right) W_f(x) \\ = |e_\varepsilon| (|w_{f_z}(x)| - W_{f_z}(x)) \leq 0 \end{aligned} \quad (41)$$

$$\begin{aligned} |U w_{g_z}(x) u_{eq_z}| |e_\varepsilon| - U e_\varepsilon \text{sat}\left(\frac{e_s}{\varepsilon}\right) W_{g_z}(x) |u_{eq_z}| = \\ \begin{cases} U |e_\varepsilon| (|w_{g_z} u_{eq_z}| - W_{g_z} |u_{eq_z}|) \leq 0 & \text{if } U \geq 0 \\ |U| |e_\varepsilon| (|w_{g_z} u_{eq_z}| + W_{g_z} |u_{eq_z}|) \leq 0 & \text{if } U < 0 \end{cases} \end{aligned} \quad (42)$$

$$\begin{aligned} \dot{V}_z = -\gamma e_\varepsilon^2 + |e_\varepsilon| (|w_{f_z}(x)| - W_{f_z}(x)) \\ + |u_{eq_z}| |e_\varepsilon| (|U w_{g_z}(x)| - U W_{g_z}(x)) \end{aligned} \quad (43)$$

Since $\gamma e_\varepsilon^2 \geq 0$ this shows that V_z is a non-increasing function of time.

Proposition 3 : from the Eqn. (5), the subsystems that govern the dynamics of position (x, y) is given by:

$$\begin{pmatrix} \dot{x}_9 \\ \dot{x}_{10} \end{pmatrix} = \begin{pmatrix} \dot{x} \\ u_x \frac{1}{m} U_z \end{pmatrix} \quad (44)$$

$$\begin{pmatrix} \dot{x}_{11} \\ \dot{x}_{12} \end{pmatrix} = \begin{pmatrix} \dot{y} \\ u_y \frac{1}{m} U_z \end{pmatrix} \quad (45)$$

The following proposed indirect fuzzy adaptive control u_x and u_y Eqn. (46):

$$\begin{aligned} u_x &= \frac{\hat{n}}{U_z} (x_d^{(n)} + \gamma e_{\varepsilon_x} + \bar{e}_{sx}) + \eta_x(x) \text{sat}\left(\frac{e_{sx}}{\varepsilon}\right) \\ u_y &= \frac{\hat{n}}{U_z} (y_d^{(n)} + \gamma e_{\varepsilon_y} + \bar{e}_{sy}) + \eta_y(x) \text{sat}\left(\frac{e_{sy}}{\varepsilon}\right) \end{aligned} \quad (46)$$

Ensure the stability toward the desired trajectory asymptotically.

Where $\eta_x(x) = \frac{1}{g_{05}} (+W_{g_5}(x) |u_{eq}|)$ and $\eta_y(x) = \frac{1}{g_{06}} (+W_{g_6}(x) |u_{eq}|)$ with $W_{g_5}(x)$ and $W_{g_6}(x)$ are the known bounds of approximation errors of functions: g_5 and g_6 respectively.

proof : for the subsystem that govern the variable x , we have : $\hat{g} = \frac{1}{m} \rightarrow u_x \frac{1}{m} U_1 = u_x \hat{g}_x U_z$ and by the choice of the candidate function of Lyapunov V_i where $i = \{x, y\}$:

$$V_i = \frac{1}{2} e_{\varepsilon_i}^2 + \frac{1}{2\eta_f} \tilde{\theta}_{f_i}^T \tilde{\theta}_{f_i} + \frac{1}{2\eta_g} \tilde{\theta}_{g_i}^T \tilde{\theta}_{g_i}$$

its derivative is given by :

$$\begin{aligned} \dot{V}_i &= \left(U_z \tilde{\theta}_g^T \phi_g x u_{eq_i} - U_z w_g(x) u_{eq_i} - U_1(g_x) u_{s_i} \right) e_\varepsilon \\ &+ \frac{1}{\eta_g} \tilde{\theta}_g^T \dot{\theta}_g - \gamma e_\varepsilon^2 \end{aligned} \quad (47)$$

We take the following adaptation law: $\dot{\theta}_g(t) = -\eta_g \varphi_g(x) e_{\varepsilon_x} u_{eq} U_z$

If the parameter g_i is constant, so the adaptation law for the position controller is : $\dot{\theta}_g(t) = -\eta_g e_{\varepsilon_x} u_{eq_i} U_z$

$$\begin{aligned} \dot{V}_i &= \left(U_z \tilde{\theta}_g^T \phi_g(x) u_{eq_i} - U_1 w_g(x) u_{eq_i} - U_z(g(x)) u_{s_i} \right) e_\varepsilon \\ &- \gamma e_\varepsilon^2 - U_z \tilde{\theta}_g^T \varphi_g(x) e_\varepsilon u_{eq_i} \\ \Rightarrow \dot{V}_i &\leq -\gamma e_\varepsilon^2 + (-U_z w_g(x) u_{eq_i} - U_z(g(x)) u_{s_i}) e_\varepsilon \end{aligned} \quad (48)$$

To ensure that the equation Eqn. (48) being less or equal to zero, we choose u_s as follow:

$$u_{s_x} = \frac{g_i}{g_{0_i}} (W_{g_i}(x) |u_{eq_i}|) \text{sat}\left(\frac{e_{s_x}}{\varepsilon}\right)$$

We constate that : $-(+w_g(x)u_{eq_i})e_\varepsilon \leq (+|w_g(x)u_{eq_i}|)|e_\varepsilon|$ so :

$$\begin{aligned} \dot{V}_i &= \left(-U_1 w_g(x)u_{eq_i} - U_z \left(\frac{g_i}{g_{0_i}}\right) (W_{g_i}(x)|u_{eq_i}|) \text{sat}\left(\frac{e_s}{\varepsilon}\right)\right) e_\varepsilon \\ &\quad - \gamma e_\varepsilon^2 + \\ \dot{V}_i &\leq -\gamma e_\varepsilon^2 + (|U_z w_g(x)u_{eq_i}|)|e_\varepsilon| \\ &\quad - U_z e_\varepsilon \left(\frac{g_i}{g_{0_i}} (W_{g_i}(x) |u_{eq_i}|) \text{sat}\left(\frac{e_s}{\varepsilon}\right)\right) \end{aligned} \quad (49)$$

With : $(\frac{g_i}{g_{0_i}}) \geq 1, U_z \geq 0, |w_{f_i}(x)| \leq W_{f_i}(x)$ and $|w_{g_i}(x)| \leq W_{g_i}(x)$ then $\forall e_s \neq 0$ we have

$$\begin{aligned} \dot{V}_i &= \\ &\quad -\gamma e_\varepsilon^2 + |U_z w_{g_i}(x)u_{eq_i}| |e_\varepsilon| - U_z e_\varepsilon \text{sat}\left(\frac{e_s}{\varepsilon}\right) W_{g_i}(x) |u_{eq_i}| \\ &= U_z |e_\varepsilon| (|w_{g_i}(x)u_{eq_i}| - W_{g_i}(x) |u_{eq_i}|) \leq 0 \\ \dot{V}_i &\leq -\gamma e_\varepsilon^2 \end{aligned} \quad (50)$$

since $\gamma e_\varepsilon^2 \geq 0$, this shows that V_i , is a nonincreasing function of time.

The correspondent's angles are given by the two following equations Eqn. (51):

$$\begin{aligned} \phi_d &= \arcsin(u_x \sin \psi_d - u_y \cos \psi_d) \\ \theta_d &= \arcsin\left(\frac{1}{\cos \phi} (u_x \cos \psi_d - u_y \sin \psi_d)\right) \end{aligned} \quad (51)$$

for $\psi \cong 0$ we can approximate the Eqn. (51) using the following approximations: $\cos \psi_d \approx 1$ and $\sin \psi_d \approx 0 \Rightarrow \phi_d = \arcsin(-u_y)$ and $\theta_d = \arcsin(\frac{1}{\cos \phi} u_x)$

5 Results and discussions

To verify the reliability and robustness of the controller with simulations of tracking in the presence of different disturbance levels, considering the results obtained using the proposed control in Section 4.2 and considering the various trajectories where we use a sampling step of 0.01 and $W_{f_i} = 0.1$ for $i = \{\phi, \theta, \psi\}$ and $W_{g_j} = 0.1$ for $j = \{\phi, \theta, \dots, y, z\}$ and $\gamma = 10$ for attitude and altitude control, while $\gamma = 2$ and $K = [5, 1]$ for position control.

5.1 Simulation with Disturbance

5.1.1 Attitude Control:

this test is about applying our proposed control to quadrotor to study its behavior in addition to its performances. Take the following trajectory:

$$\begin{cases} \theta_d(t) = \sin(t); \varphi_d(t) = \sin(t + \pi) \\ \psi_d(t) = 0.2 \quad z_d(t) = 1 \end{cases} \quad \forall t$$

The desired and the real angles of output (in radians) are presented in Fig. 11, and the sliding errors are presented in Fig. 12.

For a complicated trajectory, we choose the following desired signal:

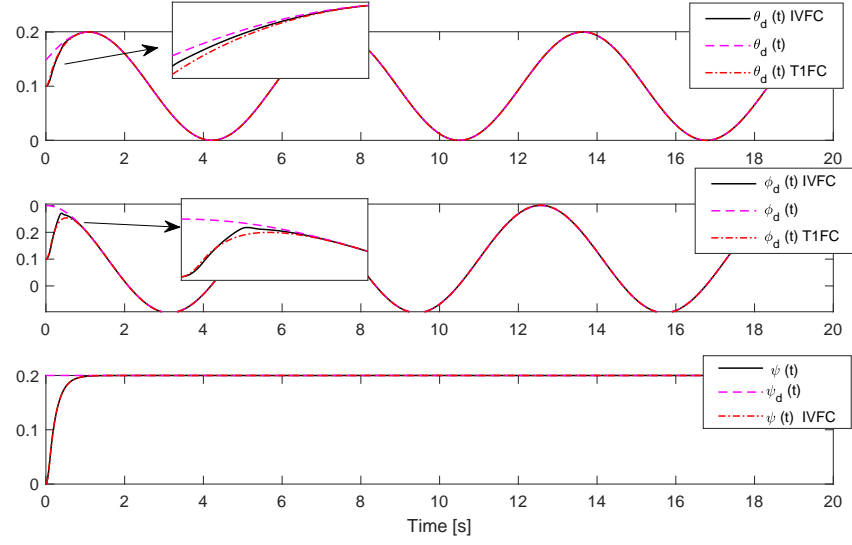
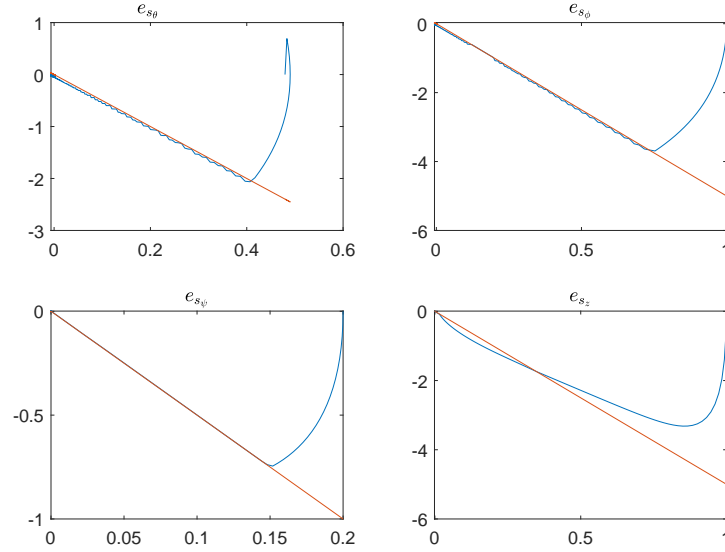


Figure 11: Responses of system with a sinusoidal trajectory

Figure 12: sliding errors e_s

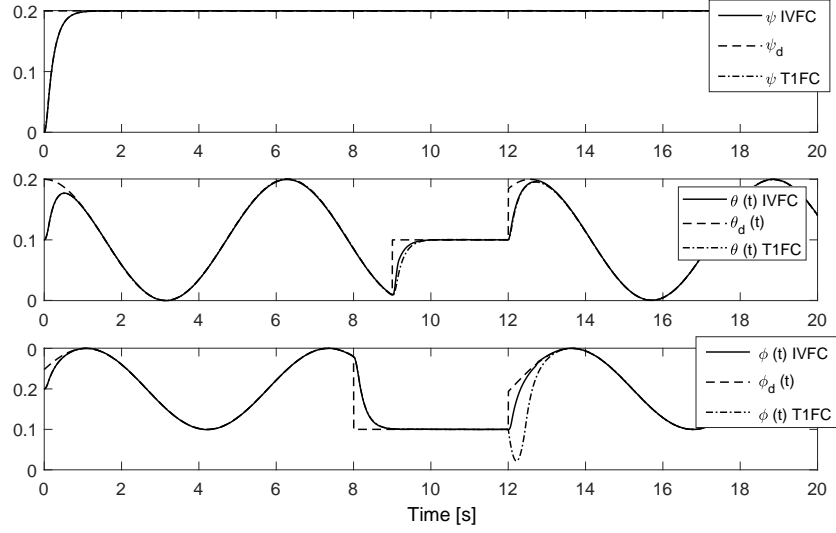
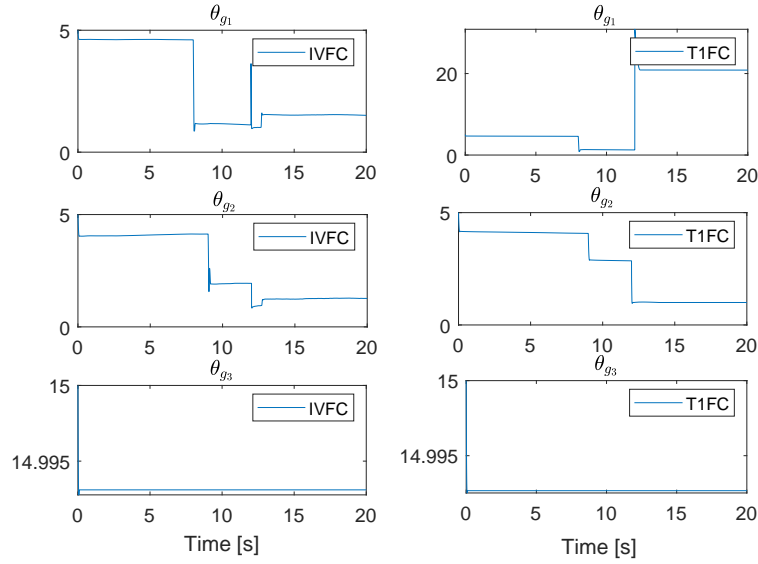


Figure 13: Responses of system with a sinusoidal trajectory

Figure 14: Adaptations of Parameters $\theta_{g\phi}$, $\theta_{g\theta}$ and $\theta_{g\psi}$ in function of time: a)T1FC b)IVFC

$$[\theta_d(t), \varphi_d(t), z_d(t), \psi_d(t)] = \begin{cases} [0, 0, 1, 0.2] & \text{if } t \in [10, 12] \\ [\sin(t), \sin(t + \pi), 1, 0.2] & \text{otherwise} \end{cases} \quad (52)$$

desired angles and real angles of the system's output (in radians) are shown in Fig. 13 .

The figures Fig. 14 and Fig. 15 depict the evolution of the fuzzy model's adaptation parameters. It is clear that parameters converge rapidly to their stationary values. Those peaks are due to system perturbations.

We note that the system met the desired reference. The error of tracking in Fig. 13 and the Table 3 can be explained by the error between the estimated model and the real model. Anyway, the effect of this error is too small, and we note that the error obtained with this approach is minimal.

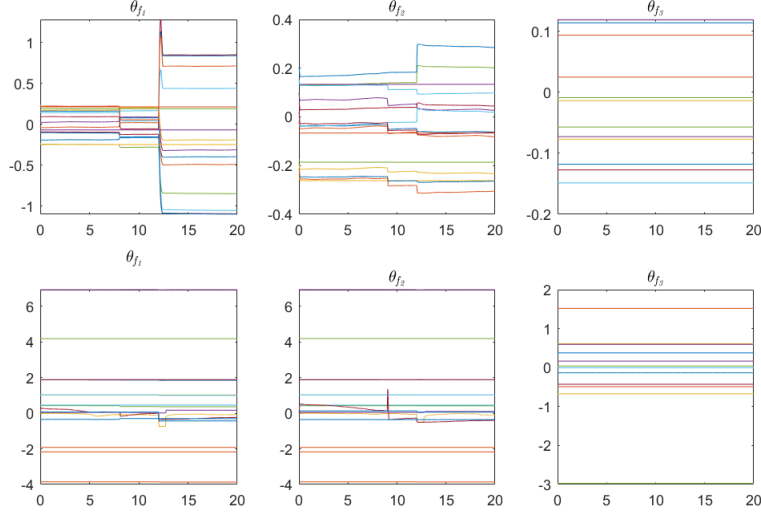
Figure 15: Parameters adaptation θ_{f_ϕ} , θ_{f_θ} and θ_{f_ψ} in function of time: a)T1FC b)IVFC

Table 3: Comparison of MSE between T1 and IVFC

MSE	IVFC	T1FC
θ	22.5090	23.0242
$\tilde{\beta}$	44.9816	81.8549
$\tilde{\psi}$	1.0554	1.0587

5.1.2 Position Control:

we consider the following trajectory:

$$x_d(t) = \sin(t), y_d(t) = \sin(t + \pi), z_d(t) = 1, \psi_d(t) = 0.2$$

In the absence of any parametric variation in the case of position tracking, the results of simulation are almost identical and sufficiently acceptable Fig. 16. Figure Fig. 17 depicts the angles that correspond to position responses.

5.2 Simulation with Perturbation

5.2.1 Attitude Control:

This test is about the application of the control law to a quadrotor with perturbations in the range of time [12s,14s]. This test is carried out by varying δI and δJ_r around the values of the rotor's inertia J_r and the drone's inertia (I_{xx}, I_{yy}, I_{zz}). The variation can be written as $\hat{J}_r = J_r + \delta J_r$ and $\hat{I} = I + \delta I$.

Figures (Fig. 18 19 and 20) show the results of tracking for the three tests mentioned above. In the case where we introduce the model disturbance, we note a deviation from the desired consign.

Note that in all simulations, the added perturbations are quickly compensated by the controller IVFC proposed with respect to the conventional type-1 controller. Note also that in Table 4 the rejection of perturbation is more effective, especially when the system has a high level of disturbance.

5.2.2 Position Control:

In this simulation, the model is submitted to an external disturbance on the angles φ_d and θ_d that attack the position controller. This additive perturbation is chosen to be $\delta\varphi = 0.25rad$ in the range [8s 8.5s] and $\delta\theta = 0.25rad$ in the range [9s 9.5s], as shown in the Fig. 22. The tracking response of position is shown in Fig. 23 .

The results of Fig. 23 and the MSE Table 5 show the efficiencies and robustness of the proposed control.

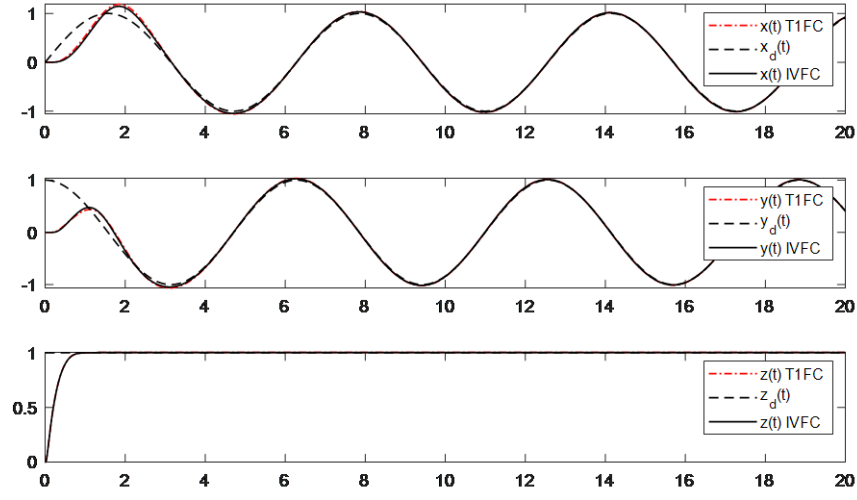


Figure 16: response of system with sinusoidal trajectory

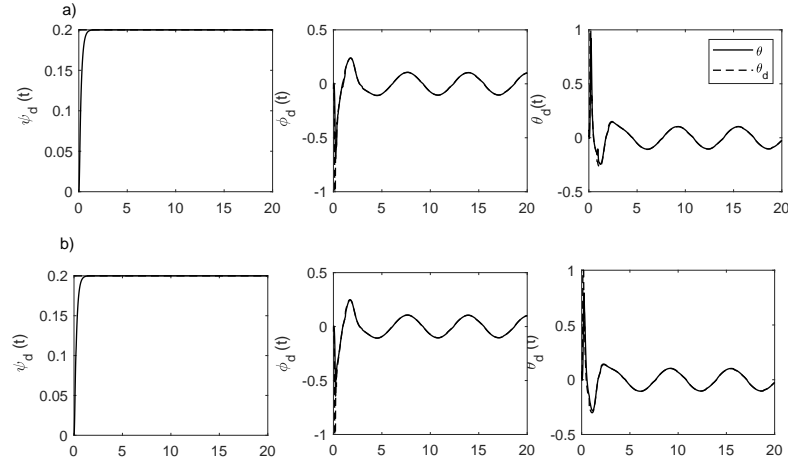
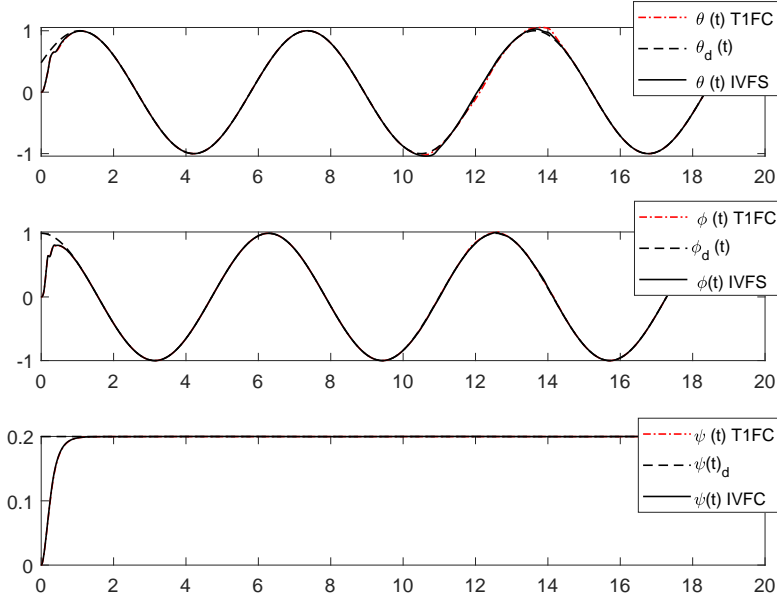
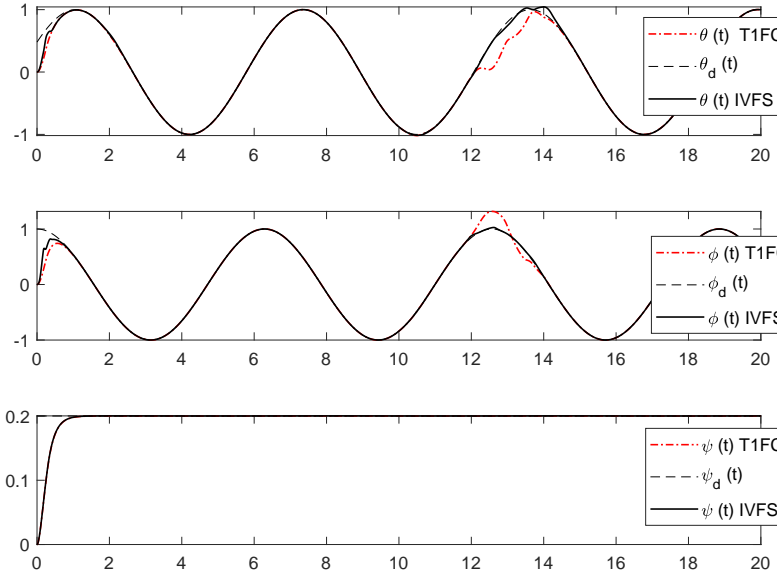


Figure 17: correspondent's Angles to responses of position a) T1FC b) IVFC

Table 4: Comparison of MSE between T1 and IVFC

	test 1		test 2		test 3	
MSE	IVFC	T1FC	IVFC	T1FC	IVFC	T1FC
$\tilde{\theta}$	7.492	13.216	7.590	9.693	8.060	9.118
$\tilde{\beta}$	17.548	49.829	17.310	32.508	17.295	31.033
$\tilde{\psi}$	1.055	1.056	1.055	1.055	1.055	1.053

Figure 18: Adaptive Sliding mode control in presence of disturbance $\delta J_r = 10\% J_r$ Figure 19: Adaptive Sliding mode control in presence of disturbance $\delta J_r = 15\% J_r$

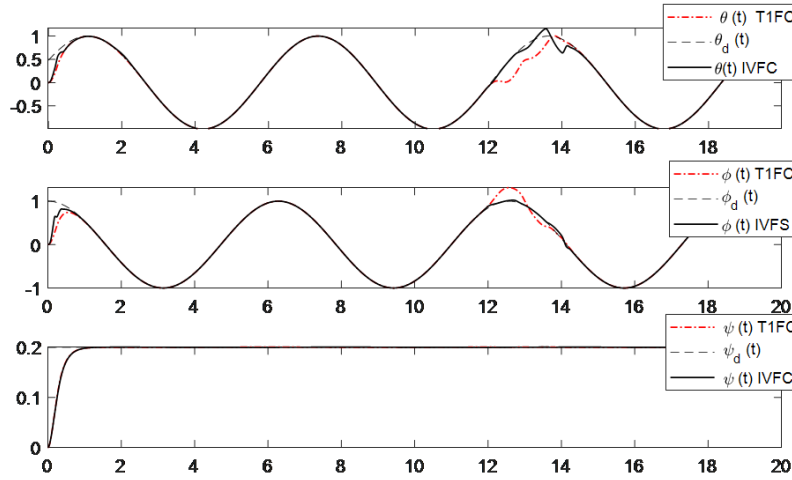


Figure 20: Adaptive sliding mode controller in presence of perturbations $\delta J_r = 20\%J_r$

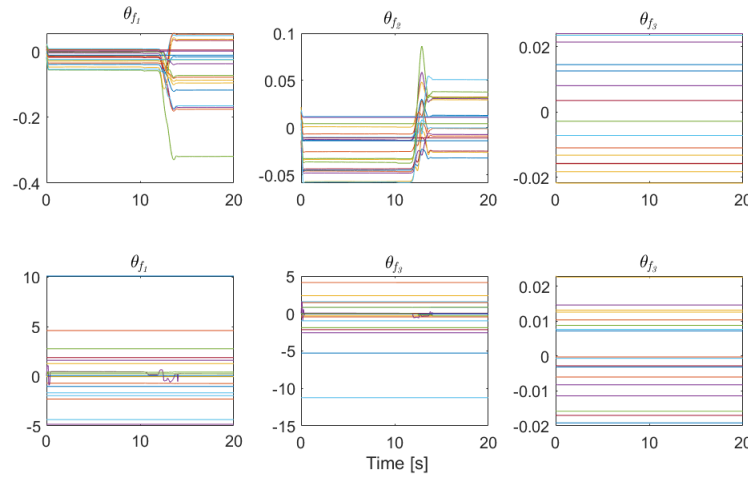


Figure 21: Evolution of Adaptations parameters of $f_i(x)$: a) T1FC b) IVFC

6 CONCLUSION

In this paper, we presented an algorithm to build an IVFM fuzzy model from input-output data for a nonlinear system. The proposed method for constructing the Takagi-Sugeno (TS) type-2 fuzzy model, based on input-output data of the identified dynamics, is constructed by identifying the structure using fuzzy clustering, then, the envelope detection, and finally the identification of parameters. The proposed method is used to model the unknown parts of the quadrotor dynamics, and the model is then used to design a fuzzy sliding mode adaptive controller in which the unknown dynamics are approximated by an IVFM as an initial model, and the model is then adjusted online using Lyapunov theory-based law. The compared results are presented to demonstrate the effectiveness of the proposed method. Many cases are considered for the sake of showing and testing the performance of tracking and robustness. Finally, the results show that the tracking error has converged despite internal and external disturbances.

References

H.Mo and Gh. Farid. Nonlinear and adaptive intelligent control techniques for quadrotor uav. *Journal Name*, 21(2): 989–1008, March 2019.

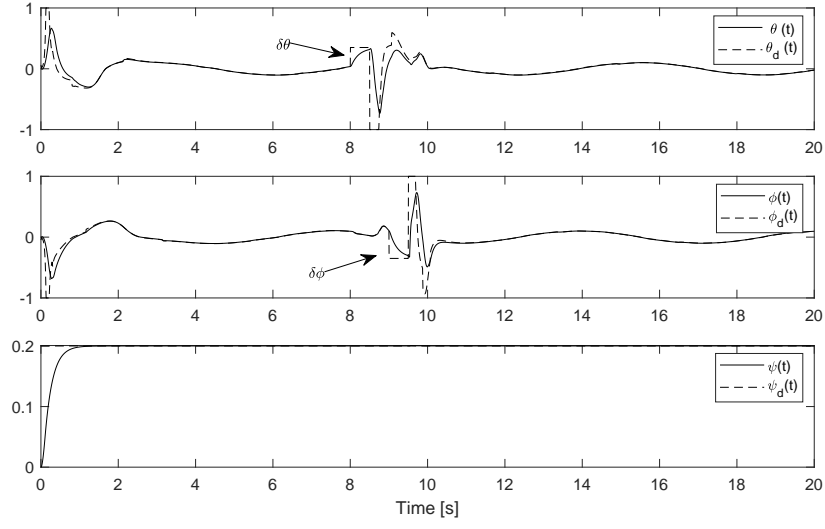


Figure 22: Angles correspondent with perturbation $\delta\varphi = \delta\theta = 0.25\text{rad}$

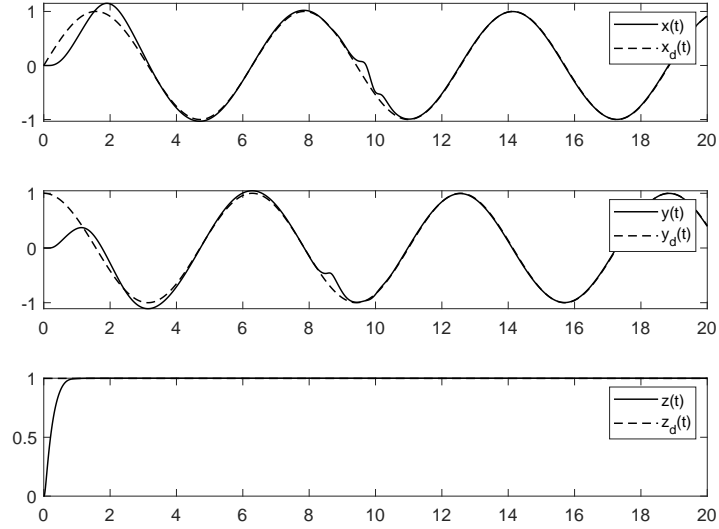


Figure 23: Response of system using sliding mode adaptative fuzzy model based

Table 5: Comparison of MSE between T1 and IVFC

MSE	T1FC	IVFC
\tilde{x}	46.6442	39.7494
\tilde{y}	127.3148	123.8104
\tilde{z}	30.7955	30.7955

- H. and Gao, D. Guo C. Liu, and J. Liu. Fuzzy adaptive pd control for quadrotor helicopter. *IEEE Int. Conf. Cyber Technol. Automation Control Intell. Syst. Shenyang, China*, 1(5):281–286, May 2015.
- A. Rabhi, M. Chadli, and C. Pegard. Robust fuzzy control for stabilization of a quadrotor. *15th Int. Conf. Adv. Robotics, Tallinn, Estonia*, 1(5):471–475, May 2011.
- F. J. and A. Fakharian Niroumand and M. S. Seyedsajadi. Fuzzy integral backstepping control approach in attitude stabilization of a quadrotor uav. *13th Iranian Conf. Fuzzy Syst., Qazvin, Iran*, 1(5):1–6, May 2013.
- M. Pazooki and A. H. Mazinan. Hybrid fuzzybased sliding-mode control approach, optimized by genetic algorithm for quadrotor unmanned aerial vehicles. *Complex Intell. Syst.*, 1(5):1–3, May 2017.
- A. Li M. Umer Khan S. Shamshirband Ul Amin, R. and A. Kamsin. An adaptive trajectory tracking control of four rotor hover vehicle using extended normalized radial basis function network. *Mech. Syst. Signal Process.*, 83:53–74, 2017.
- T. Dierks and S. Jagannathan. Output feedback control of a quadrotor uav using neural networks. *IEEE Trans. Neural Netw.*, 21:50–66, 2010.
- T. Dierks and S. Jagannathan. Neural network control of quadrotor uav formations. *Amer. Control Conf., St. Louis, MO, USA*, 1(5):2990–2996, May 2009.
- Y. Wang J. Tan Li, S. and Y. Zheng. Adaptive rbfnns/integral sliding mode control for a quadrotor aircraft. *Neurocomputing*, 216(5):126–134, May 2016.
- S. and Kwak S. and You K. Lee, K. and Kim. Quadrotor stabilization and tracking using nonlinear surface sliding mode control and observer. *Appl. Sci.*, 11(5):1–3, May 2021.
- R. Babuska, J.A. Roubos, and H.B. Verbruggen. Identification of mimo systems by input–output ts fuzzy models. *IEEE Int. Conf. on Fuzzy Sysys, Anchorage, AK, USA*, 1(5):657–662, 1998.
- R. Babuska and H.B. Verbruggen. Constructing fuzzy models by product space clustering. *H. Hellendoorn, D. Driankov (Eds.), Fuzzy Model Identification, Selected Approaches, Springer-Verlag*, 1(5):53–90, May 1997.
- D.E. Gustafson and W.C. Kessel. Hybrid fuzzybased sliding-mode control approach, optimized by genetic algorithm for quadrotor unmanned aerial vehicles. *Fuzzy clustering with a fuzzy covariance matrix, Proc. IEEE CDC, San Diego, CA*, 1(5):761–766, May 1979.
- O.D. Filho and G.L. Serra. Evolving fuzzy clustering algorithm based on maximum likelihood with participatory learning,. *IEEE (EAIS)*, 1:1–3, May 2016.
- M. Bouhentala, M. Ghanai, and Kh. Chafaa. Interval-valued membership function estimation for fuzzy modeling. *Fuzzy Sets and Systems*, 361:101–113, June 2017. doi:doi.org/10.1016/j.fss.2018.06.008.
- S. Bouabdallah. *design and control of quadrotors with application to autonomous flying*. PhD Thesis, Lausanne, EPFL, 2007.
- S.S Sastry and A. Isidori. Adaptive control of linearizable systems,. *IEEE Trans. Automat. Contr.*, 34:1123–1131, Nov 1989.
- J-J E Slotine and Coetsee. Adaptive sliding controller synthesis for nonlinear systems. *Int. J. Control*, 43(6):1631–1651, 1986.